Published in final edited form as:
J Immunol. 2014 April 15; 192(8): 3958–3968. doi:10.4049/jimmunol.1301533.

Innate PI3K p110δ regulates Th1/Th17 development and microbiota-dependent colitis

Erin C. Steinbach[*,†], **Taku Kobayashi**[†], **Steven M. Russo**[†], **Shehzad Z. Sheikh**[†], **Gregory R. Gipson**[*,†], **Samantha T. Kennedy**[*,†], **Jennifer K. Uno**[†,‡], **Yoshiyuki Mishima**[†], **Luke B. Borst**[§], **Bo Liu**[†], **Hans Herfarth**[†], **Jenny P. Y. Ting**[*], **R. Balfour Sartor**[*,†], and **Scott E. Plevy**[*,†]

[*]Department of Microbiology and Immunology, University of North Carolina School of Medicine, Chapel Hill, NC 27599, USA

[†]Center for Gastrointestinal Biology and Diseases, Department of Medicine, University of North Carolina School of Medicine, Chapel Hill, NC 27599, USA

[‡]Department of Biology, Elon University, Elon, NC 27244, USA

[§]Department of Pathology, College of Veterinary Medicine, North Carolina State University, Raleigh, NC USA

Abstract

The p110δ subunit of class I_A phosphoinositide 3-kinase modulates signaling in innate immune cells. We previously demonstrated that mice harboring a kinase-dead p110δ subunit ($p110\delta^{KD}$) develop spontaneous colitis. Macrophages contributed to the Th1/Th17 cytokine bias in $p110\delta^{KD}$ mice through increased IL-12 and IL-23 expression. Here, we show that the enteric microbiota is required for colitis development in germ free $p110\delta^{KD}$ mice. Colonic tissue and macrophages from $p110\delta^{KD}$ mice produce significantly less IL-10 compared to wild type (WT) mice. $p110\delta^{KD}$ APC co-cultured with naïve $CD4^+$ antigen-specific T cells also produce significantly less IL-10, and induce more IFN-γ- and IL-17A-producing $CD4^+$ T cells compared to WT APC. Illustrating the importance of APC – T cell interactions in colitis pathogenesis *in vivo*, *Rag1*$^{-/-}$/$p110\delta^{KD}$ mice develop mild colonic inflammation and produced more colonic IL-12p40 compared to *Rag1*$^{-/-}$ mice. However, $CD4^+CD45RB^{high/low}$ T cell *Rag1*$^{-/-}$/$p110\delta^{KD}$ recipient mice develop severe colitis with increased percentages of IFN-γ- and IL-17A-producing lamina propria $CD3^+CD4^+$ T cells compared to *Rag1*$^{-/-}$ recipient mice. Intestinal tissue samples from patients with Crohn's disease reveal significantly lower expression of *PIK3CD* compared to intestinal samples from non-IBD control subjects ($p<0.05$). *PIK3CD* expression inversely correlated with the ratio of *IL12B:IL10* expression. In conclusion, the PI3K subunit p110δ controls homeostatic APC – T cell interactions by altering the balance between IL-10 and IL-12/23. Defects in p110δ expression

Corresponding Author: Scott E. Plevy, M.D., Vice President, IBD Disease Area Stronghold, Janssen R&D, 1400 McKean Road, Mailstop 32-3-2, Spring House, PA 19477, splevy@its.jnj.com, Office Phone: 215-793-7558, Fax: 215-986-1022.

Contribution of Authors: Study concept and design (ECS, TK, SZS, SEP); Acquisition of data (ECS, TK, SMR, GRG, JKU, YM, SEP); Analysis and interpretation of data (ECS, TK, SMR, SZS, GRG, JKU, YM, LBB, SEP); Drafting of the manuscript (ECS, SEP); Critical revision of the manuscript for important intellectual content (ECS, TK, SZS, SEP); Statistical analysis (ECS, SEP); Obtained funding (ECS, HH, JP-YT, RBS, SEP); Technical or material support (YM, LBB, BL, HH, JP-YT, RBS); Study supervision (RBS, SEP).

and/or function may underlie the pathogenesis of human IBD and lead to new therapeutic strategies.

Keywords

Monocytes/Macrophages; Mucosa; Cytokines; Inflammation; Th1/Th2 Cells

INTRODUCTION

Genetic variants that confer susceptibility to the human inflammatory bowel diseases Crohn's disease (CD) and ulcerative colitis highlight the importance of innate immune interactions with the enteric microbiota in both initiating and controlling inflammation (1). Commensal and pathogenic microorganisms are recognized through conserved molecular microbial patterns by pattern-recognition receptors, of which toll-like receptors (TLRs) form integral components (2). Although mechanisms by which the host distinguishes commensal from pathogenic bacteria are not well defined, under normal conditions TLR signaling initiated by the enteric microbiota is protective (3). Phosphoinositide 3-kinases (PI3Ks) have emerged as important regulators of TLR signaling (4, 5). Class I_A PI3Ks have five different regulatory subunits and three p110 catalytic subunits: p110α and p110β are expressed ubiquitously in many tissues whereas p110δ is enriched in leukocytes (6). Agents that activate macrophages to produce IL-12p40, the common subunit of the proximal inflammatory cytokines IL-12 and IL-23, also activate Class I_A PI3K (7). Activation of PI3K in turn blocks the expression of IL-12p40 mRNA (*Il12b*) (7). Although inflammatory responses are essential for eradicating pathogenic microbes, excessive/prolonged activation of innate immunity is harmful to the host. PI3K-mediated negative feedback of IL-12p40 is important to prevent excessive innate immune responses.

The clearest role of PI3K in chronic inflammation is described in a mouse harboring a kinase-dead p110δ catalytic subunit of PI3K ($p110\delta^{D910A/D910A}$ kinase-dead; here on referred to as "$p110\delta^{KD}$") (8). These mice demonstrate B and T cell defects including defective antigen receptor signaling and impaired humoral responses. Notably, the occurrence of spontaneous colitis was demonstrated in PI3K $p110\delta^{KD}$ mice (9). Expression of IL-12p40, Th1 and Th17 cytokines was described in the intestinal and systemic immune compartments. Consistent with a homeostatic role for p110δ in the intestine, wild type (WT) mice raised in a germ free (GF) environment markedly upregulated colonic p110δ (*Pik3cd*) expression when the enteric microbiota were introduced, but colitis-prone *Il10*$^{-/-}$ mice did not (9).

Given the role of the PI3K p110δ subunit in innate immune processes fundamental to the pathogenesis of IBD, host-enteric microbiota and APC – T cell interactions in $p110\delta^{KD}$ mice were further characterized. We describe a requirement for the enteric microbiota to drive intestinal inflammation in $p110\delta^{KD}$ mice. Microbial-innate immune interactions, through p110δ, maintain homeostasis through regulation of both protective (IL-10) and inflammatory (IL-12p40) cytokines. Furthermore, p110δ orchestrates innate regulation of adaptive immune responses. Importantly, in human CD, decreased intestinal *PIK3CD* gene

expression is demonstrated which inversely correlates with intestinal *IL12B:IL10* ratios. Thus, p110δ appears to be a central homeostatic switch in the intestine, governing the critical balance between microbiota-induced IL-12/23 and IL-10, shaping the subsequent T cell response. Counter to prevailing paradigms where p110δ inhibition is a strategy in inflammatory diseases (10, 11), induction of p110δ could be a potential therapeutic approach in human IBD.

MATERIALS AND METHODS

Mice

All mice were maintained on a C57BL/6 background in conventional or GF housing. PI3K p110$\delta^{D910A/D910A}$ (p110δ^{KD}) mice were previously obtained from Dr. Bart Vanhaesebroeck (Queen Mary University of London, London, England). GF p110δ^{KD} mice were Caesarian derived as previously described (12) and were maintained according to standard techniques in the University of North Carolina National Gnotobiotic Resource Center. OT-II (C57BL/6-Tg(TcraTcrb)425Cbn/J) male mice were provided by JPY Ting (UNC, Chapel Hill). All animal experiments were in compliance with protocols approved by the International Animal Care and Use Committee of the University of North Carolina at Chapel Hill.

Reagents

LPS from *Escherichia coli* was purchased from Invivogen (San Diego, CA). Zymosan A from *Saccharomyces cerevisiae* was purchased from Sigma (St. Louis, MO). Inhibitors IC87114, Rapamycin, and SB-216763 were purchased from Selleck Chemicals (Houston, TX). Cecal bacterial lysates (CBL) C57BL/6 mice were prepared as described previously (13). The peptide corresponding to residues 323-339 of ovalbumin (OVA) was purchased from AnaSpec (Fremont, CA).

Colonic Tissue Explant Culture

Colonic tissue explant cultures were performed as described previously (14).

Histology

Slides were prepared for H&E staining and a pathologist (L.B.B.) blinded to the study groups performed histological analysis using established criteria for p110δ^{KD} mice (9). In T cell adoptive transfer studies, the following scoring system was utilized: Tissue changes were categorized into inflammatory and epithelial changes and graded for severity (0= normal, 1= mild, 2= moderate, 3= marked and 4= severe); the sum of the two grades comprises the histopathology score. For inflammation, a score of 0 (normal) signified rare small lymphoplasmacytic aggregates confined to the lamina propria; scores of 1 (mild) and 2 (moderate) represented increasing numbers of multifocal inflammatory aggregates which were predominantly confined to the lamina propria, with occasional submucosal infiltration; a score of 3 (marked) was assigned if inflammatory infiltrates frequently extended into the submucosa and muscular layers; a score of 4 (severe) was designated if transmural inflammation was common. Epithelial changes, characterized by hypertrophy, were scored (0-4) with increasing severity and prevalence of the observed change.

Cell Isolation

Bone marrow-derived macrophages (BMDMs) were cultured as described previously (15). Splenocytes were isolated as described (16) and further separated into $CD11c^+$ and $CD11c^-$/$Cd11b^+$ cells by MACS with anti-CD11c and anti-CD11b microbeads (Miltenyi Biotec, Auburn, CA). Lamina propria mononuclear cells (LPMCs) were isolated from mouse colons as described previously (17). LPMCs were further separated into $CD11b^+$ and $CD11b^-$ cells by MACS with anti-CD11b microbeads (Miltenyi Biotec, Auburn, CA).

Cell culture experiments

BMDMs or splenocytes were cultured at 1×10^6/ml in the presence of LPS (1 ng/ml), Zymosan A (10 μg/ml), or PBS, and supernatants were harvested after 4 hours or 24 hours (BMDMs or splenocytes, respectively). Inhibitors IC87114 (0.1 or 1 μM), Rapamycin (1 or 10 μM), SB-216763 (1 or 10 μM), or DMSO were added 1 hour prior to stimulation with LPS or Zymosan A. $CD11b^+$ LPMCs were treated with IC87114 (10 μM) for 30 minutes prior to exposure to heat killed *E. coli* (HKEC, MOI=100) for 3 hours. Total RNA was assessed for *Il12b* and *Il10* expression by quantitative PCR.

Western blot analysis

BMDMs were cultured at 1×10^6/ml with LPS (1 μg/ml) or cecal tissue from GF to CNV mice was collected. Cell or tissue lysates were collected in RIPA buffer with protease and phosphatase inhibitors. Equal amounts of protein were loaded and run on a 10% SDS-PAGE gel. Blots were probed for phosphorylated GSK-3β (Ser9) and total GSK-3β with antibodies from Cell Signaling Technology (Danvers, MA) and phosphorylated CREB (Ser133) (EMD Millipore, Billerica, MA) and total CREB (Santa Cruz Biotechnology, Dallas, TX).

Quantitative RT-PCR

Quantitative RT-PCR was performed on total RNA as described (14). Murine primer sequences will be provided upon request. The following human primer sequences were used:*PIK3CD*, forward, 5'-GCGCCGGGACGATAAGGAGTC-3', reverse, 5'-GCTGCCCACAGGGGTCTACCT-3'; *IL10*, forward, 5'-GCCTAACATGCTTCGAGATC-3', reverse, 5'-TGATGTGTGGGTCTTGGTTC-3'; *IL12B*, forward, 5'-GCTCTTGCCCTGGACCTGAACGC-3', reverse, 5'-CGTAGAATTGGATTGGTATCCGG-3'; *GAPDH*, forward, 5'-GGTGAAGGTCGGAGTCAACGGA-3', reverse, 5'-GAGGGATCTCGCTCCTGGAAGA-3'.

ELISAs

IL-12p40 and IL-10 (BD Biosciences, San Jose, CA) and IFN-β concentrations (R&D Systems, Minneapolis, MN) were determined by sandwich ELISA according to manufacturer's instructions.

APC-$CD4^+$ T cell Co-culture

Splenic APCs from WT or $p110\delta^{KD}$ mice were isolated by negative selection using CD90.2 microbeads (Miltenyi Biotec, Auburn, CA). Splenic APCs were incubated overnight with

CBL (50 ng/ml), and, after washing several times to remove extracellular antigen, APC were co-cultured with negatively-selected $CD4^+$ T cells (CD8α/B220/MHC II microbeads, Miltenyi Biotec, Auburn, CA) from WT or *Il10*$^{-/-}$ mice at a 3:2 ratio (APC:T cell) for 72 hours. For antigen specific studies, APCs were incubated overnight with LPS (10 ng/ml) and OVA peptide (323-339, 5 μM) (13). After washing to remove extracellular antigen, APC were co-cultured with negatively-selected $CD4^+$ T cells (CD8α/B220/MHC II microbeads, Miltenyi Biotec, Auburn, CA) from mice expressing a transgenic TCR that recognizes OVA epitope residues 323-339 (OT-II mice) at a 3:2 ratio (APC:T cell) for 72 hours. $CD4^+$ T cells were analyzed for intracellular cytokine expression (IFN-γ and IL-17A) by flow cytometry.

Flow Cytometry

$CD4^+$ T cells were stimulated for 4 hours with PMA (100 ng/ml) and ionomycin (1 μg/ml) in the presence of GolgiStop™ (BD Biosciences, San Jose, CA). Cells were then washed and stained with APC-conjugated anti-CD3 (Clone 17A2, eBioscience, San Diego, CA). After fixing and permeabilizing the cells with BD Cytofix/Cytoperm™ (BD Biosciences, San Jose, CA), staining for intracellular PE-conjugated anti-IFN-γ (Clone XMG1.2, eBioscience, San Diego, CA) and FITC-conjugated anti-IL-17A (Clone eBio17B7, eBioscience, San Diego, CA) was performed. Flow cytometry samples were run on a CyAn™ ADP Analyzer (Beckman Coulter, Brea, CA) and analyzed using Summit v4.3 (Beckman Coulter, Brea, CA).

$CD4^+CD45RB^{high/low}$ T cell adoptive transfer colitis

T cell mediated colitis was induced in *Rag1*$^{-/-}$ and *Rag1*$^{-/-}$/p110δ^{KD} (RKO/δ^{KD}) mice at 8 weeks of age as described previously (18). $CD4^+$ T cells were isolated by negative selection (CD8α/B220/MHC II microbeads, Miltenyi Biotec, Auburn, CA) and stained with FITC-conjugated anti-CD4 (Clone GK1.5, eBioscience, San Diego, CA) and PE-conjugated anti-CD45RB (Clone 16A, BD Pharmingen, San Jose, CA). $CD4^+$ T cells were sorted into $CD45RB^{high}$ and $CD45RB^{low}$ populations using a MoFlo™ XDP Cell Sorter (Beckman Coulter, Brea, CA). Mice were i.p. injected with 4×10^5 $CD4^+CD45RB^{high}$ cells admixed with 2×10^5 $CD4^+CD45RB^{low}$ cells as described (18). Clinical scores were assigned as described (19).

Human intestinal samples

Intestinal samples were obtained from surgical resections from CD patients and subjects requiring surgical intervention for non-inflammatory conditions (eg, colon cancer). In CD patients, when available, paired inflamed and non-inflamed intestinal segments, as determined by gross appearance by the processing pathologist, were obtained for analysis. The University of North Carolina Institutional Review Board approved collection of de-identified samples, and written informed consent was obtained from all patients.

Statistical analysis

Statistical significance for data subsets was assessed by the two-tailed Student's *t* test. p values < 0.05 were considered to be significant. All data are expressed as mean ± standard error (SEM).

RESULTS

Presence of the enteric microbiota is necessary for the development of colitis in p110δ^{KD} mice

To determine whether the microbiota is necessary for the development of colitis, p110δ^{KD} mice were derived germ free (GF). GF p110δ^{KD} mice up to 30 weeks of age did not develop histological colitis (Fig. 1A, left, Supplemental Fig. 1A). Interestingly, GF p110δ^{KD} mice produced significantly less colonic IL-10 compared to GF WT mice. GF p110δ^{KD} and WT mice were then transitioned to conventionalized housing (CNV), and colonic inflammation was assessed at days 7 and 14 after transfer. Compared to GF to CNV WT mice, colons from GF to CNV p110δ^{KD} mice demonstrated increased colitis scores (Fig. 1A, middle and right, Supplemental Fig. 1A). However, GF to CNV p110δ^{KD} mice gained weight similarly to GF to CNV WT mice (Supplemental Fig. 1B). Furthermore, colonic explants from day 7 and 14 GF to CNV p110δ^{KD} mice produced significantly less IL-10 (Fig. 1B, middle and right) compared to GF to CNV WT mice. At day 14, GF to CNV p110δ^{KD} mice produced significantly elevated IL-12p40 (Fig. 1C, middle and right) compared to WT GF to CNV mice. IL-10 is important for the maintenance of intestinal homeostasis in part through inhibition of IL-12p40 (20). The ratio of colonic IL-12p40 to IL-10 protein production therefore reflects the overall balance of intestinal pro- and anti-inflammatory cytokines. Indeed, colons from days 7 and 14 GF to CNV p110δ^{KD} mice demonstrated significantly higher ratios of IL-12p40:IL-10 production (Fig. 1D) compared to GF to CNV WT mice.

Given the recent report of co-regulation of IL-10 and IFN-β by p110δ in dendritic cells (21), we measured IFN-β levels were assessed in colonic explant tissue cultures from GF to CNV WT and p110δ^{KD} mice. Interestingly, IFN-β production was *enhanced* in colonic explants from day 7 GF to CNV p110δ^{KD} mice compared to WT mice (Fig. 1E), in contrast to decreased levels of IL-10 production in p110δ^{KD} mice. IFN-β production was increased in LPS stimulated p110δ^{KD} compared to WT BMDMs (Fig. 1F). Additionally, LPS stimulated *Il10*$^{-/-}$ BMDMs produced more IFN-β compared to WT BMDMs (Fig. 1F, right), consistent with previously reported regulation of IFN-β by IL-10 (21). To assess the direct contribution of IFN-β production from colonic macrophages, CD11b^{+} lamina propria mononuclear cells, comprising mostly macrophages, were isolated from p110δ^{KD} mice and stimulated with heat-killed *E. coli* (HKEC). Similar to BMDMs, HKEC stimulated p110δ^{KD} CD11b^{+} LPMCs produced significantly more IFN-β compared to WT CD11b^{+} LPMCs (Fig. 1G), suggesting that p110δ differentially regulates IL-10 and IFN-β in macrophages.

PI3K p110δ regulates macrophage production of IL-10 in response to PAMPs

WT and p110δ^{KD} BMDMs were exposed to TLR agonists (LPS (TLR4), 5ng/ml; Pam3CSK4 (TLR2/1), 5 ng/ml; Zymosan A (TLR2/6), 5 μg/ml), and cytokine production was measured. BMDMs from p110δ^{KD} mice produced less IL-10 in response to all TLR agonists tested compared to WT BMDMs (Fig. 2A). Additionally, p110δ^{KD} BMDMs exposed to TLR agonists produced significantly more IL-12p40 compared to WT BMDMs (Fig. 2B), in agreement with our previously published data (9). Consequently, the ratio of IL-12p40:IL-10 production in TLR ligand treated p110δ^{KD} BMDMs was consistently increased compared to WT BMDMs (Fig. 2C). LPS or Zymosan A stimulated CD11b^{+} and

CD11c^{+} splenocytes from p110δ^{KD} mice also produced less IL-10 and more IL-12p40 than WT splenic cells (Supplemental Fig. 2A-D).

To further validate these findings, LPS stimulated WT BMDMs were treated with p110 isoform-specific chemical inhibitors. LPS activated WT BMDMs demonstrated a dose-dependent decrease in IL-10 production (Fig. 3A, left) and increase in IL-12p40 (Fig. 3B, left) with specific chemical inhibition of p110δ (IC87114). Interestingly, p110δ inhibition in WT BMDMs markedly enhanced IL-12p40 production above levels produced by p110δ^{KD} BMDMs. It is possible that there is compensation by other PI3K isoforms in p110δ^{KD} BMDMs but not in chemically inhibited WT BMDMs. Indeed, we have previously shown that phosphorylation of Akt in LPS stimulated p110δ^{KD} BMDMs is not completely abrogated (9). PI3K p110α- and p110β inhibition (PIK-90 and TGX-221, respectively) did not alter LPS stimulated IL-10 production (Supplemental Fig. 2E, F, left) or IL-12p40 (Supplemental Fig. 2G, H, left) in WT BMDMs, in agreement with reported results in dendritic cells (21). As a control, p110δ-specific inhibition of LPS-activated p110δ^{KD} BMDMs did not alter IL-10 or IL-12p40 expression (Fig. 3, right panels). However, in p110δ^{KD} BMDMs, p110β inhibition decreased IL-10 (Supplemental Fig. 2F, right) production, and p110α- or p110β-specific inhibition modestly enhanced LPS induced IL-12p40 expression (Supplemental Fig. 2G, H, right) suggesting that in the absence of p110δ function other isoforms may have modest effects on IL-10/IL-12p40 regulation.

Chemical inhibition of p110δ in *Il10*$^{-/-}$ BMDMs led to a dose-dependent increase in IL-12p40 production (Fig. 3C, right), suggesting that p110δ-mediated decreases in IL-12p40 are in part independent of the inhibitory actions of IL-10. Relevant to mucosal innate inflammatory responses, WT CD11b^{+} colonic lamina propria mononuclear cells (LPMC) treated with heat killed *E. coli* (HKEC) demonstrated diminished *Il10* (Fig. 3D) and enhanced *Il12b* (Fig. 3E) expression in the presence of the p110δ-specific inhibitor. As a control, expression of neither cytokine was altered in CD11b^{+} colonic LPMC from p110δ^{KD} mice treated with the p110δ-specific inhibitor.

mTOR and GSK-3β act downstream of p110δ in macrophages to regulate cytokine production

PI3Ks modulate multiple downstream signaling pathways, of which mammalian target of rapamycin (mTOR) and glycogen synthase kinase-3β (GSK-3β) have been previously shown to regulate cytokine secretion in macrophages (22). PI3K p110δ^{KD} BMDMs treated with LPS demonstrated impaired phosphorylation of GSK-3β and CREB (Fig. 4A and B, respectively), but not p70 S6 kinase (downstream of mTOR, data not shown). Furthermore, colonic expression of p-GSK-3β and was attenuated in GF to CNV p110δ^{KD} mice compared to GF to CNV WT mice (Fig. 4C). BMDMs from WT and p110δ^{KD} mice were exposed to mTOR or GSK-3β inhibitors (rapamycin or SB-216763, respectively) prior to LPS stimulation. Rapamycin decreased IL-10 (Fig. 5A, C) and increased IL-12p40 (Fig. 5B, D) protein and mRNA expression in WT and p110δ^{KD} TLR stimulated BMDMs. These same trends were observed in WT and p110δ^{KD} CD11b^{+} and CD11c^{+} splenocytes (Supplemental Fig. 3A-D). Inhibition of GSK-3β in p110δ^{KD} BMDMs and splenocytes increased IL-10 protein (Fig. 5E, Supplemental Fig. 3E, F) and mRNA expression (Fig. 5G), while p110δ^{KD}

BMDMs and splenocytes decreased IL-12p40 protein (Fig. 5F, Supplemental Fig. 3G) and mRNA (Fig. 5H) expression. Hence, mTOR and GSK-3β are downstream of p110δ and are relevant for regulation of IL-10 and Il-12p40.

Antigen presenting cell (APC) p110δ regulates T cell cytokine production

To begin to determine whether resident APCs regulate intestinal T cell phenotype and function, T cell cytokines and lineage markers were measured in p110δ^{KD} colons. Colonic *Tbx21* and *Rorc* transcripts (Fig. 6A, B, middle and right), the hallmark transcription factors of Th1 (23) and Th17 cells (24), respectively, were increased in GF to CNV p110δ^{KD} mice at days 7 and 14 post-transition compared to matched GF to CNV WT mice. Likewise, increased *Ifng* and *Il17a* transcripts (Fig. 6C, D, middle and right) were detected in cecal tissue from days 7 and 14 GF to CNV p110δ^{KD} compared to matched GF to CNV WT mice.

Consequently, we next investigated whether T cell dependent IL-12p40 and IL-10 expression was altered in p110δ^{KD} APCs. Splenic CD4^{+} T cells from WT mice were cultured with either WT or p110δ^{KD} splenic APCs pulsed with cecal bacterial lysate (CBL). CBL pulsed p110δ^{KD} APCs cultured with naïve WT CD4^{+} T cells produced decreased levels of IL-10 (Fig. 6E, middle) and increased levels of IL-12p40 (Fig. 6F, middle) compared to WT APCs. WT and p110δ^{KD} APCs cultured with *Il10*$^{-/-}$ CD4^{+} T cells demonstrate that IL-10 expression is largely derived from APCs (Fig. 6E, right). As expected, CBL pulsed p110δ^{KD} APCs also produced significantly less IL-10 (Fig. 6E, left) and more IL-12p40 (Fig. 6F, left) compared to WT APCs in the absence of CD4^{+} T cells.

Next, to study antigen-specific APC-T cell interactions, splenic CD4^{+} T cells from OVA specific transgenic T cell receptor mice (OT-II mice) were co-cultured with OVA pulsed and LPS activated WT and p110δ^{KD} APCs. OVA-loaded p110δ^{KD} APCs induced significantly more IFN-γ- (Fig. 6H, I) and IL-17A-producing (Fig. 6H, J) CD4^{+} T cells compared to OVA-loaded WT APCs (Fig. 6G, I, J). However, T cell proliferation was induced to a similar extent by both WT and p110δ^{KD} APCs (Supplemental Fig. 4A-C). These data suggest that cytokine production by p110δ^{KD} APCs directs differentiation of antigen specific Th1 and Th17 CD4^{+} T cells.

These results suggest a model where defective p110δ, through regulation of IL-10 and IL-12p40, leads to inflammatory effector T cell development. To test this model *in vivo*, we generated *Rag1*$^{-/-}$/p110δ^{KD} mice (RKO/δ^{KD}). Interestingly, colitis is present but attenuated in the absence of an adaptive immune system (Fig. 7A, B). Colonic explant cultures from RKO/δ^{KD} mice produced significantly decreased IL-10 (Fig. 7C) and increased IL-12p40 (Fig. 7D) compared to colonic tissue explant cultures from *Rag1*$^{-/-}$ mice.

It was previously reported that p110δ^{KD} CD4^{+} T cells adoptively transferred into *Rag1*$^{-/-}$ recipients induce colitis owing to impaired T regulatory cell function (25). To study how p110δ inactivation in non-lymphocyte populations affects T cell differentiation, admixed WT CD4^{+}CD45RB^{high} and CD4^{+}CD45RB^{low} T cells were adoptively transferred into *Rag1*$^{-/-}$ and RKO/δ^{KD} mice (CD45RB recipient mice) and monitored for colitis development. Adoptive transfer of T cells demonstrated reconstitution, with localization of CD3^{+} cells to the colons of recipient mice (Supplemental Fig. 4D). Total body weight of

recipient mice was recorded until the experiment was terminated at day 24 due to severe clinical manifestations in the CD45RB recipient RKO/δ^{KD} mice. There was no difference in weight loss between CD45RB recipient *Rag1*$^{-/-}$ or RKO/δ^{KD} mice (data not shown). Clinical colitis activity scores (Fig. 8A) and quantitative colonic histologic analysis (Fig. 8B, C) from CD45RB recipient RKO/δ^{KD} mice were increased compared to the respective recipient *Rag1*$^{-/-}$ mice. Colonic IL-10 production was significantly lower (Fig. 8D) and IL-12p40 production higher (Fig. 8E) in CD45RB recipient RKO/δ^{KD} mice compared to CD45RB recipient *Rag1*$^{-/-}$ mice. Consequently, ratios of colonic IL-12p40:IL-10 production from CD45RB recipient RKO/δ^{KD} mice were significantly higher (Fig. 8F) than ratios from recipient *Rag1*$^{-/-}$ mice. Furthermore, more IFN- γ-producing (Fig. 8G), but not IL-17A-producing (Fig. 8H), CD4^{+} T cells were isolated from mesenteric lymph nodes (MLNs) of CD45RB recipient RKO/δ^{KD} mice compared to recipient *Rag1*$^{-/-}$ mice. Finally, a greater percentage of lamina propria CD3^{+}CD4^{+} T cells from recipient RKO/δ^{KD} mice produced IFN- γ (Fig. 8I) and IL-17A (Fig. 8J, each data point represents 3 pooled samples), compared to recipient *Rag1*$^{-/-}$ mice.

Intestinal *PIK3CD* expression correlates with *IL12B:IL10* ratios from patients with CD

Expression of p110δ (*PIK3CD*), IL-12p40 (*IL12B*) and IL-10 (*IL10*) mRNA was determined in human intestinal tissue from control subjects without intestinal inflammation and patients with CD. Significantly higher levels of *PIK3CD* mRNA were detected in non-inflamed intestinal samples from control subjects compared to tissue from patients with CD (Fig. 9A). Paired macroscopically inflamed and non-inflamed intestinal resections from the same subject were obtained from 14 CD patients. There was lower expression of *PIK3CD* in inflamed intestinal tissues compared to non-inflamed tissues obtained from the same patient (Fig. 9B). Furthermore, ratios of *IL12B:IL10* expression from individual CD patients demonstrated a strong and statistically significant inverse correlation with *PIK3CD* expression (Fig. 9C).

DISCUSSION

We previously described the development of spontaneously occurring Th1 and Th17 mediated colitis in p110δ ^{KD} (9). In the present series of experiments, we further elucidate intestinal host-microbial and APC-T cell interactions mediated by p110δ. Colitis in p110δ^{KD} mice is dependent on host responses to the enteric microbiota, as has been described in other murine colitis models (26). In the absence of the enteric microbiota, p110δ^{KD} mice did not develop intestinal inflammation, whereas after reconstitution with commensal enteric microbiota, colons from p110δ^{KD} mice demonstrated histological inflammation, impaired IL-10 and increased IL-12p40 production (Fig. 1). Consequently, altered IL-10 and IL-12p40 production by p110δ^{KD} APCs in response to microbial products and cognate interactions with T cells orchestrate pathogenic adaptive immune responses contributing to intestinal inflammation.

Class I_A PI3Ks regulate macrophage and dendritic cell responses to bacteria (5). Taken together, our results and those of others (21) elucidate a model where p110δ is an intracellular integrator of environmental signals that is involved in the restoration of

inflammatory responses to homeostasis, mediated in part by IL-10. Regulation of IL-10 expression involves both PI3K-dependent and independent pathways. Moreover, IL-10 signaling in macrophages has been shown to activate the PI3K pathway (27). Indeed, we have shown that colonic p110δ expression is attenuated in colitis-prone *Il10*$^{-/-}$ mice, suggesting that IL-10 regulation of IL-12p40 occurs in part via induction of p110δ (9). Our current and previous findings (9) demonstrate that bacterial products and IL-10 induce p110δ gene expression in macrophages, and suggest that transcription regulation of p110δ can determine functional immunologic consequences. Most studies have focused on post-translational regulation of p110δ (21, 28, 29) as the sole biologic determinant of function. Thus, transcriptional regulation of p110δ expression in macrophages may have unexpected biological significance and needs to be further explored.

Aksoy *et al*. recently demonstrated that p110δ signaling in dendritic cells dampens responses to LPS by sequestering TLR4 signaling components and facilitating the switch from toll-interleukin 1 receptor (TIR) domain containing adaptor protein (TIRAP)/MyD88 dependent inflammatory cytokine production (IL-12, IL-6, TNF-α) to TIR domain containing adaptor inducing interferon-β (TRIF)-related adaptor molecule (TRAM)/TRIF dependent anti-inflammatory cytokine production (IFN-β, IL-10) (21). It is possible that LPS induced p110δ signaling in macrophages also facilitates the switch to TRAM-TRIF signaling, leading to the enhanced production of IL-10 and IFN-β. Indeed, this agrees with our finding that p110δ^{KD} macrophages produce less LPS induced IL-10. However, we have previously shown that CD11b^{+} LPMCs from *Trif*$^{-/-}$ mice produce higher levels of basal and bacterially stimulated IL-10 compared to WT mice (30, 31). Conversely, BMDMs from *Trif*$^{-/-}$ mice produce less LPS-induced IL-10 compared to WT mice (32). These findings suggest that the TRIF pathway negatively regulates IL-10 production uniquely in intestinal macrophages. Furthermore, CD11b^{+} LPMCs produce high levels of IL-10 in GF conditions (30), suggesting that microbial signals are not necessary for driving constitutive expression of IL-10. However, TLR signaling, perhaps through the recognition of endogenous ligands, remains vital for IL-10 production in intestinal macrophages, as HKEC stimulated *MyD88*$^{-/-}$ CD11b^{+} LPMCs do not produce detectable levels of IL-10 (30). Additionally, our data suggest that IFN-β and IL-10 demonstrate differential regulation in CD11b^{+} LPMCs, in contrast to the recent study demonstrating convergent regulation in LPS stimulated BMDCs (21). Indeed, Kaiser *et al*. demonstrated cell type-specific differences in IL-10 and IFN-β production in response to LPS: BMDMs and splenic macrophages did not make detectable amounts of IFN-β but made significant amounts of IL-10 in response to LPS, whereas BMDCs produced both IFN-β and IL-10 (33), suggesting that macrophages utilize distinct pathways to regulate IFN-β and IL-10. Thus, further studies are necessary to elucidate specific intestinal macrophage signaling pathways required for IL-10 production.

In macrophages, mTOR and GSK-3β are central regulators of IL-12p40 and IL-10 downstream of PI3K. Bacterial products induce MyD88 dependent PI3K activation, leading to phosphorylation of its downstream effector molecule Akt. Akt inactivates tuberous sclerosis complex (TSC), a negative regulator of mTOR (34). Both Akt and PI3K dependent mTOR activation modulate IL-12p40 and IL-10 production by suppressing GSK-3β activity (22, 35). GSK-3β constitutively represses IL-10 by blocking cAMP response element-

binding (CREB) binding to and activation of the *Il10* promoter (36). PI3K- and mTOR-mediated inhibition of GSK-3β thus releases IL-10 from suppression by GSK-3β (36). Interestingly, mTOR activation targets were not altered in LPS stimulated p110δ^{KD} BMDCs compared to WT BMDCs, suggesting that compensatory activation pathways sustain mTOR signaling in p110δ^{KD} BMDCs (21). Indeed, mTOR is activated through many pathways, including cellular energy sensing and Wnt signaling (37). Additionally, the balance of IL-10 and IL-12p40 production, as well as other cytokines, is regulated by MAPK signaling downstream of TLR signaling (38). We previously reported that TLR-activated p110δ^{KD} macrophages demonstrate impaired Akt phosphorylation and enhanced phosphorylation of p38 and JNK MAPK, but not ERK1/2, compared to WT macrophages (9). Here we show impaired phosphorylation of the downstream mediators GSK-3β and CREB in TLR-stimulated p110δ^{KD} macrophages and in colons from GF to CNV p110δ^{KD} mice. Furthermore, other cytokines such as TNF-α are affected by p110δ, which regulates tubule fusion in TNF-α containing vesicles bound for secretion (39). Indeed, we have previously shown dysregulation of IL-12p70, IL-23, and NO in TLR-activated p110δ^{KD} macrophages (9). Thus, p110δ may regulate cytokine secretion in multiple ways. Here we showed that inhibition of GSK-3β rescues LPS induced IL-10 production in p110δ^{KD} BMDMs (Fig. 5). Our results therefore suggest that GSK-3β activity may be a therapeutic target in IBDs to induce IL-10 production. Indeed, GSK-3β inhibition has previously been shown to ameliorate colitis in mice (40).

PI3K p110δ^{KD} B and T lymphocytes demonstrate impaired proliferative signaling through the B cell and T cell receptors (8). PI3K p110δ^{KD} mice demonstrate impaired intrinsic T regulatory cell function, and p110δ^{KD} CD4^{+}CD45RB^{low} cells co-transferred with colitogenic WT CD4^{+}CD45RB^{high} cells did not protect *Rag1*$^{-/-}$ mice from T cell-mediated colitis (25). To determine how APC p110δ influences T cell subset differentiation and colitis development, APC-CD4^{+} T cell co-culture experiments (Fig. 6) were performed. CD4^{+} T cells induced greater production of IL-12p40 by APCs, while APCs from p110δ^{KD} mice induced more antigen-specific IFN-γ- and IL-17A-producing T cells. Because only WT CD4^{+} T cells were used in co-culture with APCs from both WT and p110δ^{KD} mice, T cell phenotype can be attributed to the defect in p110δ^{KD} APCs. As an *in vivo* correlate, *Rag1*$^{-/-}$ and RKO/δ^{KD} mice were reconstituted with admixed WT CD4^{+}CD45RB^{high} and CD45RB^{low} T cells (Fig. 8). Compared to respective recipient *Rag1*$^{-/-}$ mice, RKO/δ^{KD} recipient mice demonstrated significantly increased clinical and histology scores. More IFN-γ-producing T cells were isolated from mesenteric lymph nodes and colonic lamina propria of RKO/δ^{KD} recipient mice compared to recipient *Rag1*$^{-/-}$ mice. IL-17 producing CD4^{+} T cells are rarely found in MLN and other secondary lymphoid tissues but are found in abundant quantities at mucosal surfaces (41). Indeed, RKO/δ^{KD} recipient mice contained significantly higher percentages of IL-17A-producing T cells in the colonic lamina propria compared to the respective *Rag1*$^{-/-}$ recipient mice. We previously showed that bacterially stimulated p110δ^{KD} macrophages produce significantly more IL-23, a cytokine necessary for the differentiation and maintenance of Th17 cells (9).

While the development of pathogenic CD4^{+} T cells in CD45RB recipient mice was explored, we did not study Treg cell differentiation and function. During GF to CNV

transition, colons from p110δ^{KD} mice demonstrated significantly increased transcription of *Foxp3*, correlating with increased inflammation, compared to colons from WT mice (data not shown). However, this finding does not rule out functional defects in p110δ^{KD} Treg cells. It is entirely possible, and in fact likely, akin to human IBD pathogenesis, that innate and adaptive immune defects interact to drive colitis.

Interestingly, in the absence of T cells, RKO/δ^{KD} mice developed mild histopathologic colonic inflammation. The development of mild colonic inflammation in RKO/δ^{KD} mice could be explained by the presence non-*hepaticus Helicobacter* species in our mouse colony (data not shown). The ability of *H. hepaticus* to induce innate immune driven colonic inflammation in the absence of adaptive immune cells has been well described (42, 43).

Recently, p110δ inhibition has been targeted for the treatment of chronic rejection of tissue transplants, systemic lupus erythematosus, and certain lymphoid cell malignancies (10, 11, 44). While preliminary clinical results are promising, this study highlights a potentially untoward consequence of p110δ inhibition – enhanced intestinal and innate inflammatory processes initiated by APCs.

Supplementary Material

Refer to Web version on PubMed Central for supplementary material.

Acknowledgments

We thank Dr. Bart Vanhaesebroeck for providing p110δ^{KD} mice (8).

Grant support: NIH RO1 DK054452 (SEP), NIH F30 DK089692 (ECS), UNC Center for Gastrointestinal Biology and Disease P30 DK34987 (Histology Core, Gnotobiotic Core, and Immunotechnologies Core).

References

1. Rioux JD, Xavier RJ, Taylor KD, Silverberg MS, Goyette P, Huett A, Green T, Kuballa P, Barmada MM, Datta LW, Shugart YY, Griffiths AM, Targan SR, Ippoliti AF, Bernard EJ, Mei L, Nicolae DL, Regueiro M, Schumm LP, Steinhart AH, Rotter JI, Duerr RH, Cho JH, Daly MJ, Brant SR. Genome-wide association study identifies new susceptibility loci for Crohn disease and implicates autophagy in disease pathogenesis. Nat Genet. 2007; 39:596–604. [PubMed: 17435756]
2. Abreu MT. Toll-like receptor signalling in the intestinal epithelium: how bacterial recognition shapes intestinal function. Nat Rev Immunol. 2010; 10:131–144. [PubMed: 20098461]
3. Rakoff-Nahoum S, Paglino J, Eslami-Varzaneh F, Edberg S, Medzhitov R. Recognition of commensal microflora by toll-like receptors is required for intestinal homeostasis. Cell. 2004; 118:229–241. [PubMed: 15260992]
4. Liew FY, Xu D, Brint EK, O'Neill LA. Negative regulation of toll-like receptor-mediated immune responses. Nat Rev Immunol. 2005; 5:446–458. [PubMed: 15928677]
5. Fukao T, Koyasu S. PI3K and negative regulation of TLR signaling. Trends Immunol. 2003; 24:358–363. [PubMed: 12860525]
6. Koyasu S. The role of PI3K in immune cells. Nat Immunol. 2003; 4:313–319. [PubMed: 12660731]
7. Fukao T, Tanabe M, Terauchi Y, Ota T, Matsuda S, Asano T, Kadowaki T, Takeuchi T, Koyasu S. PI3K-mediated negative feedback regulation of IL-12 production in DCs. Nat Immunol. 2002; 3:875–881. [PubMed: 12154357]

8. Okkenhaug K, Bilancio A, Farjot G, Priddle H, Sancho S, Peskett E, Pearce W, Meek SE, Salpekar A, Waterfield MD, Smith AJ, Vanhaesebroeck B. Impaired B and T cell antigen receptor signaling in p110delta PI 3-kinase mutant mice. Science. 2002; 297:1031–1034. [PubMed: 12130661]
9. Uno JK, Rao KN, Matsuoka K, Sheikh SZ, Kobayashi T, Li F, Steinbach EC, Sepulveda AR, Vanhaesebroeck B, Sartor RB, Plevy SE. Altered macrophage function contributes to colitis in mice defective in the phosphoinositide-3 kinase subunit p110delta. Gastroenterology. 2010; 139:1642–1653. 1653 e1641–1646. [PubMed: 20637203]
10. Maxwell MJ, Tsantikos E, Kong AM, Vanhaesebroeck B, Tarlinton DM, Hibbs ML. Attenuation of phosphoinositide 3-kinase delta signaling restrains autoimmune disease. J Autoimmun. 2012
11. So L, Fruman DA. PI3K signalling in B- and T-lymphocytes: new developments and therapeutic advances. Biochem J. 2012; 442:465–481. [PubMed: 22364281]
12. MacDonald TT, Carter PB. Contact sensitivity in the germ-free mouse. J Reticuloendothel Soc. 1978; 24:287–293. [PubMed: 731633]
13. Cong Y, Weaver CT, Lazenby A, Elson CO. Bacterial-reactive T regulatory cells inhibit pathogenic immune responses to the enteric flora. J Immunol. 2002; 169:6112–6119. [PubMed: 12444113]
14. Hegazi RA, Rao KN, Mayle A, Sepulveda AR, Otterbein LE, Plevy SE. Carbon monoxide ameliorates chronic murine colitis through a heme oxygenase 1-dependent pathway. J Exp Med. 2005; 202:1703–1713. [PubMed: 16365149]
15. Xiong H, Zhu C, Li F, Hegazi R, He K, Babyatsky M, Bauer AJ, Plevy SE. Inhibition of interleukin-12 p40 transcription and NF-kappaB activation by nitric oxide in murine macrophages and dendritic cells. J Biol Chem. 2004; 279:10776–10783. [PubMed: 14679201]
16. Murali-Krishna K, Altman JD, Suresh M, Sourdive DJ, Zajac AJ, Miller JD, Slansky J, Ahmed R. Counting antigen-specific CD8 T cells: a reevaluation of bystander activation during viral infection. Immunity. 1998; 8:177–187. [PubMed: 9491999]
17. Kamada N, Hisamatsu T, Okamoto S, Sato T, Matsuoka K, Arai K, Nakai T, Hasegawa A, Inoue N, Watanabe N, Akagawa KS, Hibi T. Abnormally differentiated subsets of intestinal macrophage play a key role in Th1-dominant chronic colitis through excess production of IL-12 and IL-23 in response to bacteria. J Immunol. 2005; 175:6900–6908. [PubMed: 16272349]
18. Read S, Powrie F. Induction of inflammatory bowel disease in immunodeficient mice by depletion of regulatory T cells. Curr Protoc Immunol. 2001; Chapter 15(Unit 15):13. [PubMed: 18432730]
19. Maillard MH, Cotta-de-Almeida V, Takeshima F, Nguyen DD, Michetti P, Nagler C, Bhan AK, Snapper SB. The Wiskott-Aldrich syndrome protein is required for the function of CD4(+)CD25(+)Foxp3(+) regulatory T cells. J Exp Med. 2007; 204:381–391. [PubMed: 17296786]
20. Sheikh SZ, Plevy SE. The role of the macrophage in sentinel responses in intestinal immunity. Curr Opin Gastroenterol. 2010; 26:578–582. [PubMed: 20717022]
21. Aksoy E, Taboubi S, Torres D, Delbauve S, Hachani A, Whitehead MA, Pearce WP, Berenjeno-Martin I, Nock G, Filloux A, Beyaert R, Flamand V, Vanhaesebroeck B. The p110delta isoform of the kinase PI(3)K controls the subcellular compartmentalization of TLR4 signaling and protects from endotoxic shock. Nat Immunol. 2012; 13:1045–1054. [PubMed: 23023391]
22. Wang H, Brown J, Gu Z, Garcia CA, Liang R, Alard P, Beurel E, Jope RS, Greenway T, Martin M. Convergence of the mammalian target of rapamycin complex 1- and glycogen synthase kinase 3-beta-signaling pathways regulates the innate inflammatory response. J Immunol. 2011; 186:5217–5226. [PubMed: 21422248]
23. Szabo SJ, Kim ST, Costa GL, Zhang X, Fathman CG, Glimcher LH. A novel transcription factor, T-bet, directs Th1 lineage commitment. Cell. 2000; 100:655–669. [PubMed: 10761931]
24. Ivanov II, McKenzie BS, Zhou L, Tadokoro CE, Lepelley A, Lafaille JJ, Cua DJ, Littman DR. The orphan nuclear receptor RORgammat directs the differentiation program of proinflammatory IL-17+ T helper cells. Cell. 2006; 126:1121–1133. [PubMed: 16990136]
25. Patton DT, Garden OA, Pearce WP, Clough LE, Monk CR, Leung E, Rowan WC, Sancho S, Walker LS, Vanhaesebroeck B, Okkenhaug K. Cutting edge: the phosphoinositide 3-kinase p110 delta is critical for the function of CD4+CD25+Foxp3+ regulatory T cells. J Immunol. 2006; 177:6598–6602. [PubMed: 17082571]

26. Nell S, Suerbaum S, Josenhans C. The impact of the microbiota on the pathogenesis of IBD: lessons from mouse infection models. Nat Rev Microbiol. 2010; 8:564–577. [PubMed: 20622892]
27. Antoniv TT, Ivashkiv LB. Interleukin-10-induced gene expression and suppressive function are selectively modulated by the PI3K-Akt-GSK3 pathway. Immunology. 2011; 132:567–577. [PubMed: 21255011]
28. Kok K, Nock GE, Verrall EA, Mitchell MP, Hommes DW, Peppelenbosch MP, Vanhaesebroeck B. Regulation of p110delta PI 3-kinase gene expression. PLoS One. 2009; 4:e5145. [PubMed: 19357769]
29. Burke JE, Vadas O, Berndt A, Finegan T, Perisic O, Williams RL. Dynamics of the phosphoinositide 3-kinase p110delta interaction with p85alpha and membranes reveals aspects of regulation distinct from p110alpha. Structure. 2011; 19:1127–1137. [PubMed: 21827948]
30. Kobayashi T, Matsuoka K, Sheikh SZ, Russo SM, Mishima Y, Collins C, deZoeten EF, Karp CL, Ting JP, Sartor RB, Plevy SE. IL-10 regulates Il12b expression via histone deacetylation: implications for intestinal macrophage homeostasis. J Immunol. 2012; 189:1792–1799. [PubMed: 22786766]
31. Onyiah JC, Sheikh SZ, Maharshak N, Steinbach EC, Russo SM, Kobayashi T, Mackey LC, Hansen JJ, Moeser AJ, Rawls JF, Borst LB, Otterbein LE, Plevy SE. Carbon monoxide and heme oxygenase-1 prevent intestinal inflammation in mice by promoting bacterial clearance. Gastroenterology. 2013; 144:789–798. [PubMed: 23266559]
32. Boonstra A, Rajsbaum R, Holman M, Marques R, Asselin-Paturel C, Pereira JP, Bates EE, Akira S, Vieira P, Liu YJ, Trinchieri G, O'Garra A. Macrophages and myeloid dendritic cells, but not plasmacytoid dendritic cells, produce IL-10 in response to MyD88- and TRIF-dependent TLR signals, and TLR-independent signals. J Immunol. 2006; 177:7551–7558. [PubMed: 17114424]
33. Kaiser F, Cook D, Papoutsopoulou S, Rajsbaum R, Wu X, Yang HT, Grant S, Ricciardi-Castagnoli P, Tsichlis PN, Ley SC, O'Garra A. TPL-2 negatively regulates interferon-beta production in macrophages and myeloid dendritic cells. J Exp Med. 2009; 206:1863–1871. [PubMed: 19667062]
34. Weichhart T, Costantino G, Poglitsch M, Rosner M, Zeyda M, Stuhlmeier KM, Kolbe T, Stulnig TM, Horl WH, Hengstschlager M, Muller M, Saemann MD. The TSC-mTOR signaling pathway regulates the innate inflammatory response. Immunity. 2008; 29:565–577. [PubMed: 18848473]
35. Zhang HH, Lipovsky AI, Dibble CC, Sahin M, Manning BD. S6K1 regulates GSK3 under conditions of mTOR-dependent feedback inhibition of Akt. Mol Cell. 2006; 24:185–197. [PubMed: 17052453]
36. Martin M, Rehani K, Jope RS, Michalek SM. Toll-like receptor-mediated cytokine production is differentially regulated by glycogen synthase kinase 3. Nat Immunol. 2005; 6:777–784. [PubMed: 16007092]
37. Weichhart T, Saemann MD. The multiple facets of mTOR in immunity. Trends Immunol. 2009; 30:218–226. [PubMed: 19362054]
38. Bode JG, Ehlting C, Haussinger D. The macrophage response towards LPS and its control through the p38(MAPK)-STAT3 axis. Cell Signal. 2012; 24:1185–1194. [PubMed: 22330073]
39. Low PC, Misaki R, Schroder K, Stanley AC, Sweet MJ, Teasdale RD, Vanhaesebroeck B, Meunier FA, Taguchi T, Stow JL. Phosphoinositide 3-kinase delta regulates membrane fission of Golgi carriers for selective cytokine secretion. J Cell Biol. 2010; 190:1053–1065. [PubMed: 20837769]
40. Hofmann C, Dunger N, Scholmerich J, Falk W, Obermeier F. Glycogen synthase kinase 3-beta: a master regulator of toll-like receptor-mediated chronic intestinal inflammation. Inflamm Bowel Dis. 2010; 16:1850–1858. [PubMed: 20848477]
41. Atarashi K, Nishimura J, Shima T, Umesaki Y, Yamamoto M, Onoue M, Yagita H, Ishii N, Evans R, Honda K, Takeda K. ATP drives lamina propria T(H)17 cell differentiation. Nature. 2008; 455:808–812. [PubMed: 18716618]
42. Kullberg MC, Ward JM, Gorelick PL, Caspar P, Hieny S, Cheever A, Jankovic D, Sher A. Helicobacter hepaticus triggers colitis in specific-pathogen-free interleukin-10 (IL-10)-deficient mice through an IL-12- and gamma interferon-dependent mechanism. Infect Immun. 1998; 66:5157–5166. [PubMed: 9784517]
43. Kullberg MC, Rothfuchs AG, Jankovic D, Caspar P, Wynn TA, Gorelick PL, Cheever AW, Sher A. Helicobacter hepaticus-induced colitis in interleukin-10-deficient mice: cytokine requirements

for the induction and maintenance of intestinal inflammation. Infect Immun. 2001; 69:4232–4241. [PubMed: 11401959]

44. Ying H, Fu H, Rose ML, McCormack AM, Sarathchandra P, Okkenhaug K, Marelli-Berg FM. Genetic or pharmaceutical blockade of phosphoinositide 3-kinase p110delta prevents chronic rejection of heart allografts. PLoS One. 2012; 7:e32892. [PubMed: 22479345]

Abbreviations

BMDMs	bone marrow-derived macrophages
CBL	cecal bacterial lysate
CD	Crohn's disease
CNV	conventionalized
GF	germ free
GSK-3β	glycogen synthase kinase 3β
HKEC	heat killed *Escherichia coli*
LPMCs	lamina propria mononuclear cells
MLN	mesenteric lymph nodes
mTOR	mammalian target of rapamycin
p110δ^{KD}	mice with a knock-in kinase-dead p110δ subunit
RKO/δ^{KD}	*Rag1*-deficient/p110δ^{KD} mutant mice
TIRAP	toll-interleukin 1 receptor domain containing adaptor protein
TRAM	TRIF-related adaptor molecule
TRIF	toll-interleukin 1 receptor domain containing adaptor inducing interferon-β
WT	wild type

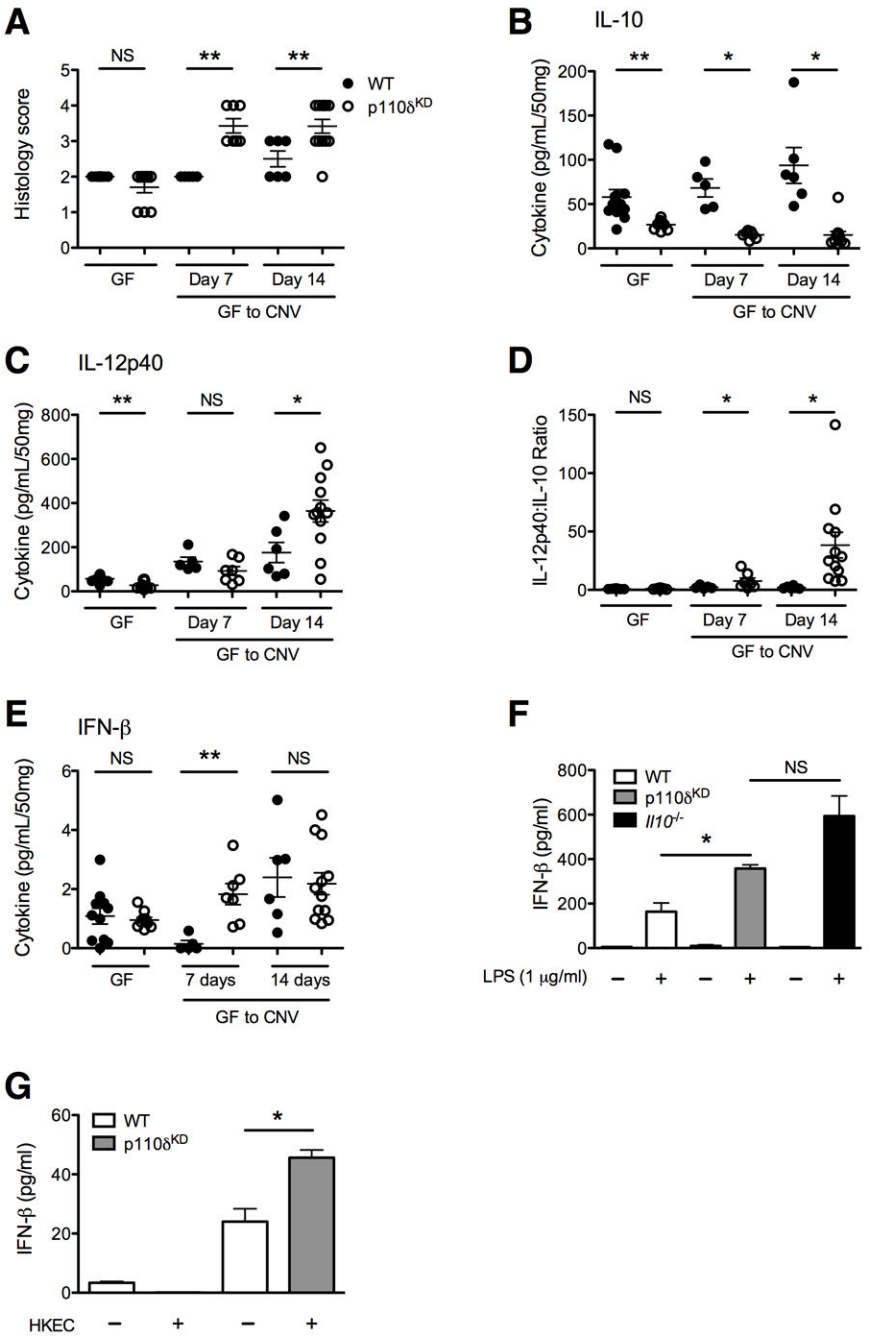

Figure 1. The enteric microbiota are required for the development of colitis in p110δ^{KD} mice

Germ-free (GF) p110δ^{KD} (n = 10) and age-matched WT (n = 12) mice were monitored for colitis up to 30 weeks of age. Additionally, GF WT and p110δ^{KD} mice were transferred to CNV housing and monitored for colitis at days 7 (n = 5 and 7, respectively) and 14 (n = 6 and 12, respectively) after transfer. (A) H&E slides of colonic tissue were scored for colitis severity using criteria described in the methods by a pathologist (L.B.B.) blinded to the experimental groups. Error bars represent mean ± SEM (NS, not significant; **, p<0.005). (B, C) Colonic tissue explants were incubated in media for 24 hours. Supernatants were

collected and assayed for IL-10 (B) and IL-12p40 (C) production by ELISA, and are expressed as the amount of cytokine (pg/ml) per 50 mg colonic tissue weight. Error bars represent mean ± SEM (NS, not significant; *, $p<0.05$; **, $p<0.005$). (D) IL-12p40 and IL-10 protein levels from colonic tissue explant cultures in individual mice were used to determine the ratio of IL-12p40 to IL-10 production. Error bars represent mean ± SEM (NS, not significant; *, $p<0.05$). (E) IFN-β protein levels from colonic tissue explant cultures were measured by ELISA and are expressed as the amount of cytokine (pg/ml) per 50 mg colonic tissue weight. Error bars represent mean ± SEM (NS, not significant; **, $p<0.005$). (F) WT, $p110\delta^{KD}$ and *Il10*$^{-/-}$ BMDMs were isolated and treated with LPS (1 μg/ml) as described in the methods. Supernatants were collected and assayed for IFN-β levels by ELISA. Error bars represent mean ± SEM from two independent experiments (NS, not significant; *, $p<0.05$). (G) WT and $p110\delta^{KD}$ $CD11b^{+}$ LPMCs were isolated as described in the methods and treated with heat-killed *E. coli* (multiplicity of infection (MOI) = 100) for 24 hours. Supernatants were collected and assayed for IFN-β levels by ELISA. Error bars represent mean ± SEM from two independent experiments (*, $p<0.05$).

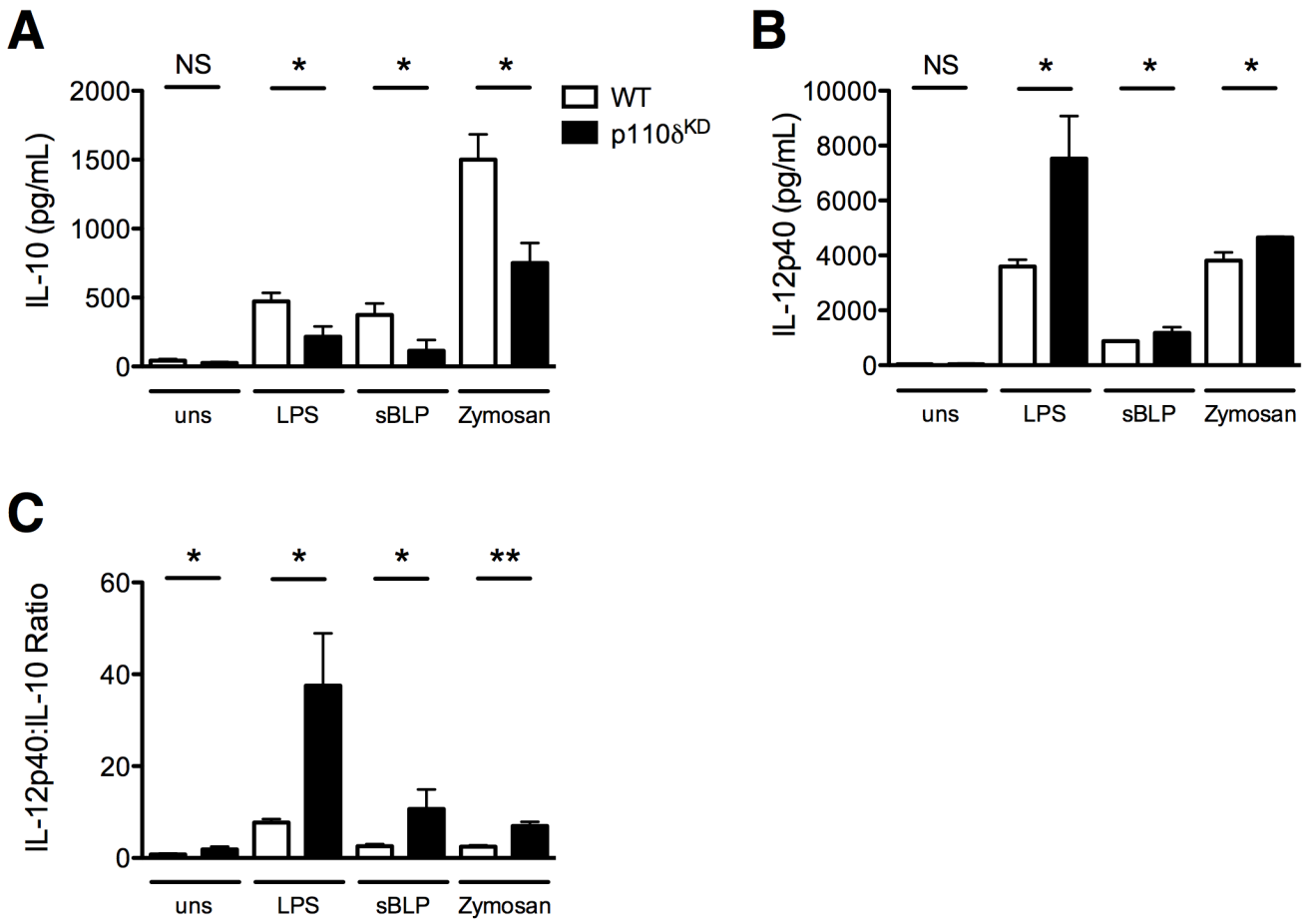

Figure 2. Defective p110δ activity alters macrophage production of IL-10 and IL-12p40 in response to bacterial products

BMDMs were stimulated with LPS (5 ng/ml), sBLP (5 ng/ml) or Zymosan A (5 μg/ml) for 8 hours. Supernatants were collected and assayed for IL-10 (A) and IL-12p40 (B) production by ELISA. Error bars represent mean ± SEM from three independent experiments (NS, not significant; *, $p<0.05$). (C) The ratio of IL-12p40 to IL-10 from individual experiments was calculated. Error bars represent mean ± SEM from three independent experiments (*, $p<0.05$; **, $p<0.005$).

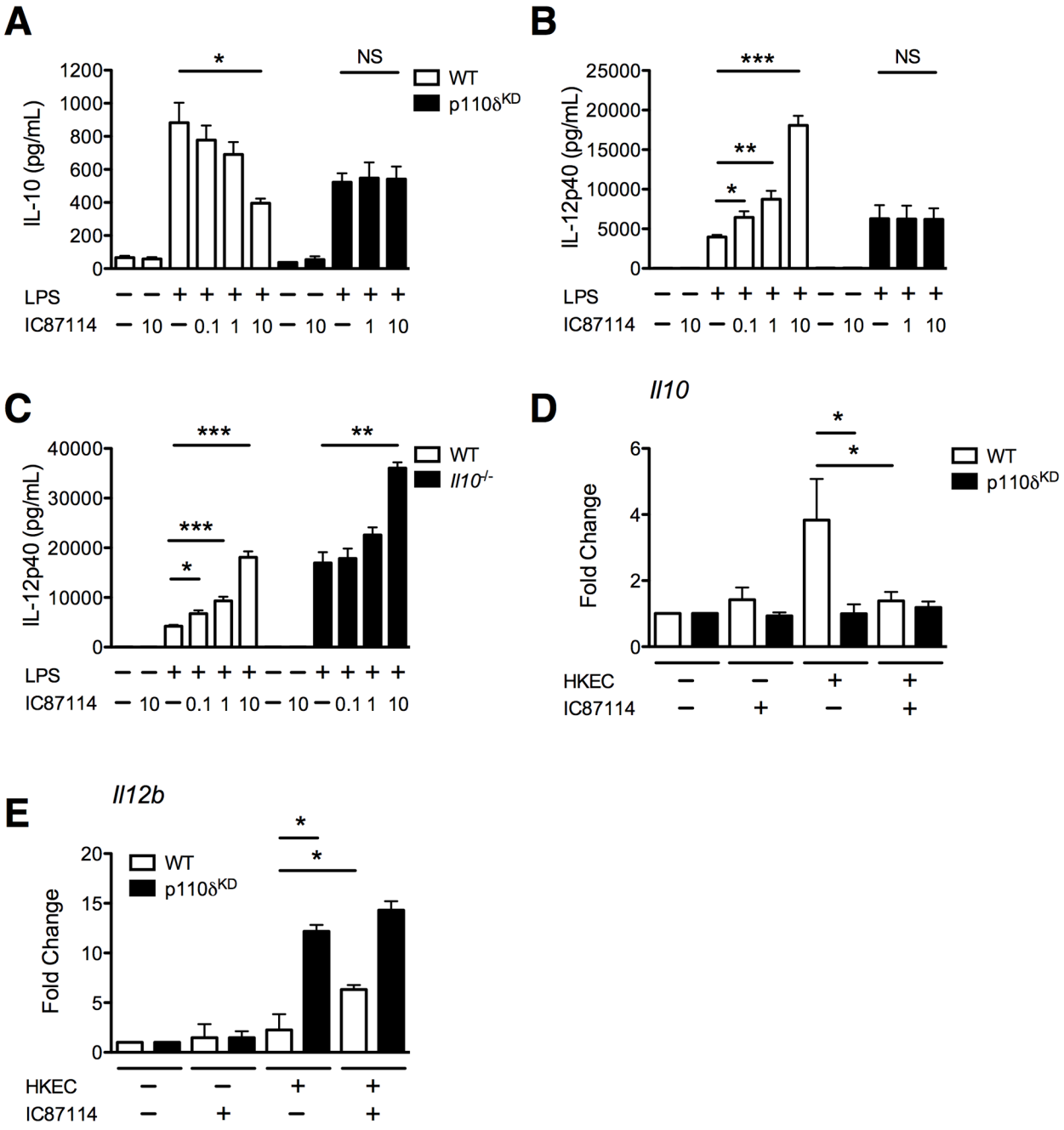

Figure 3. A p110δ-specific inhibitor decreases IL-10 and augments Il-12p40 production in WT macrophages stimulated with bacterial products

WT, p110δ^{KD} and *Il10*$^{-/-}$ BMDMs were cultured with a p110δ-specific inhibitor (IC87114, 0.1, 1 or 10 μM) for 1 hour prior to stimulation with LPS (1 ng/ml, BMDMs). Supernatants from WT and p110δ^{KD} BMDMs were collected after 8 hours of culture and assayed for IL-10 (A) and IL-12p40 (B) production by ELISA. Error bars represent mean ± SEM from three independent experiments (NS, not significant; *, p<0.05; **, p<0.005; ***, p<0.0005). (C) Supernatants from WT and *Il10*$^{-/-}$ BMDMs were collected after 8 hours of culture and assayed for IL-12p40. Error bars represent mean ± SEM from three independent

experiments (*, $p<0.05$; **, $p<0.005$; ***, $p<0.0005$). (D, E) WT and $p110\delta^{KD}$ $CD11b^{+}$ LPMCs were incubated with a p110δ-specific inhibitor (IC87114, 10 μM) 1 hour prior to stimulation with HKEC (MOI=100) for 3 hours. Quantitative RT-PCR was performed in duplicate for *Il10* (D) and *Il12b* (E) expression levels normalized to *β-actin* expression and calculated as fold induction over unstimulated cells. Error bars represent mean ± SEM for three independent experiments (*, $p<0.05$).

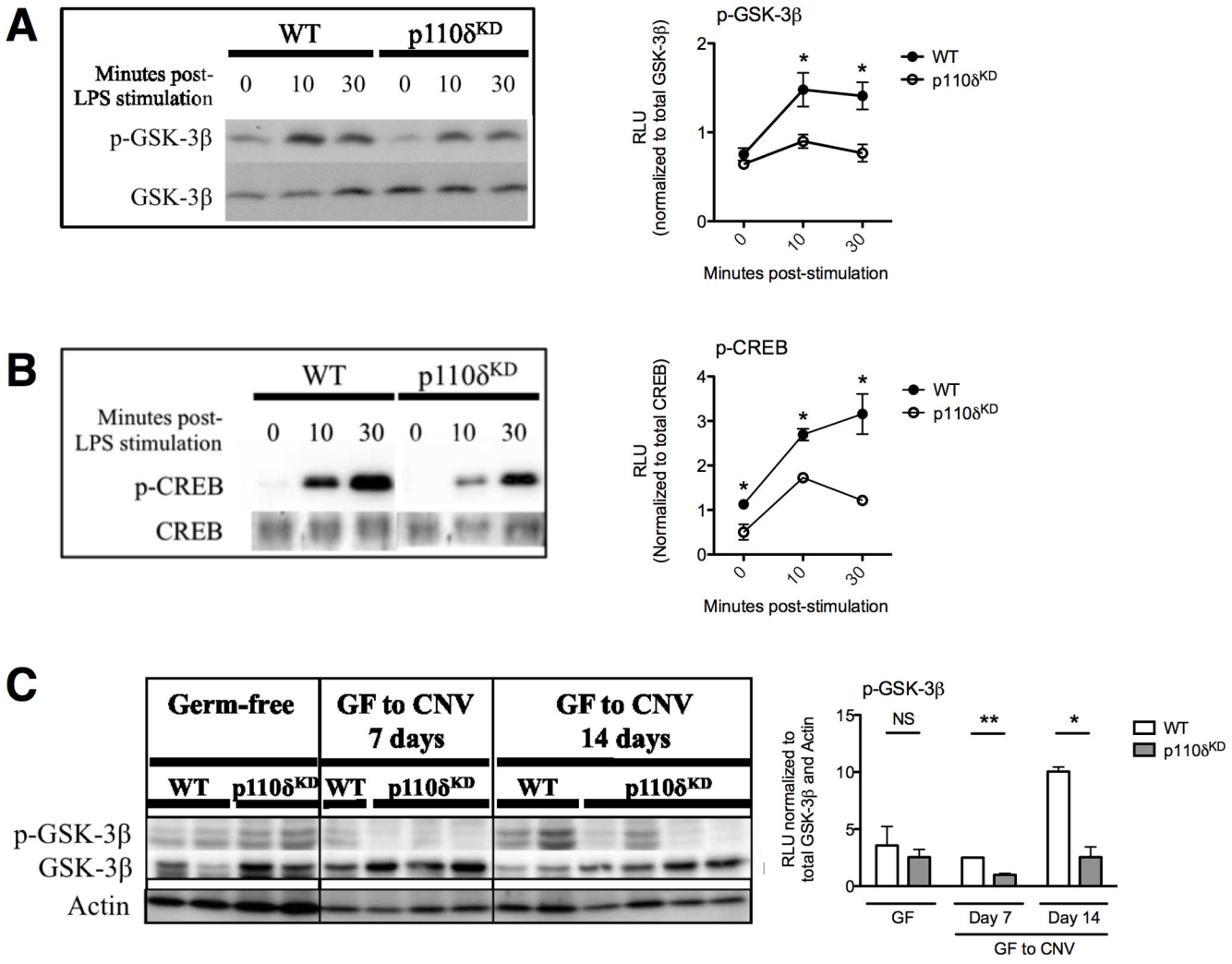

Figure 4. Phosphorylation of p110δ targets is altered in macrophages and colons from p110δ^{KD} mice

(A, B) BMDMs from WT and p110δ^{KD} mice were treated with LPS (1 μg/ml) and cell lysates were collected for western blot analysis after the indicated times. (A) Blots were probed for phosphorylated GSK-3β (Ser9) and total GSK-3β. Figure shows representative results from 3 independent experiments. Quantitative analysis of p-GSK-3β relative light units (RLU) normalized to total GSK-3β. Error bars represent mean ± SEM from three independent experiments (*, $p<0.05$ compared to WT). (B) Blots were probed for phosphorylated CREB (Ser133) and total CREB. Representative results from two independent experiments are displayed. Quantitative analysis of p-CREB relative light units (RLU) normalized to total CREB. Error bars represent mean ± SEM from three independent experiments (*, $p<0.05$ compared to WT). (C) GF WT and p110δ^{KD} mice were transferred to CNV housing and colonized with a commensal enteric microbiota (GF: WT, $n = 2$; p110δ^{KD}, $n = 2$; GF to CNV: 7 day WT, $n = 1$; 7 day p110δ^{KD}, $n = 3$; 14 day WT, $n = 2$; 14 day p110δ^{KD}, $n = 4$). Mice were sacrificed at the indicated times after colonization, and cecal tissue was collected and protein extracted. Blots were probed for the indicated

proteins/phospho-proteins. Quantitative analysis of p-GSK-3β RLU normalized to total GSK-3β and actin. Error bars represent mean ± SEM (NS, not significant; *, $p<0.05$; **, $p<0.005$ compared to WT).

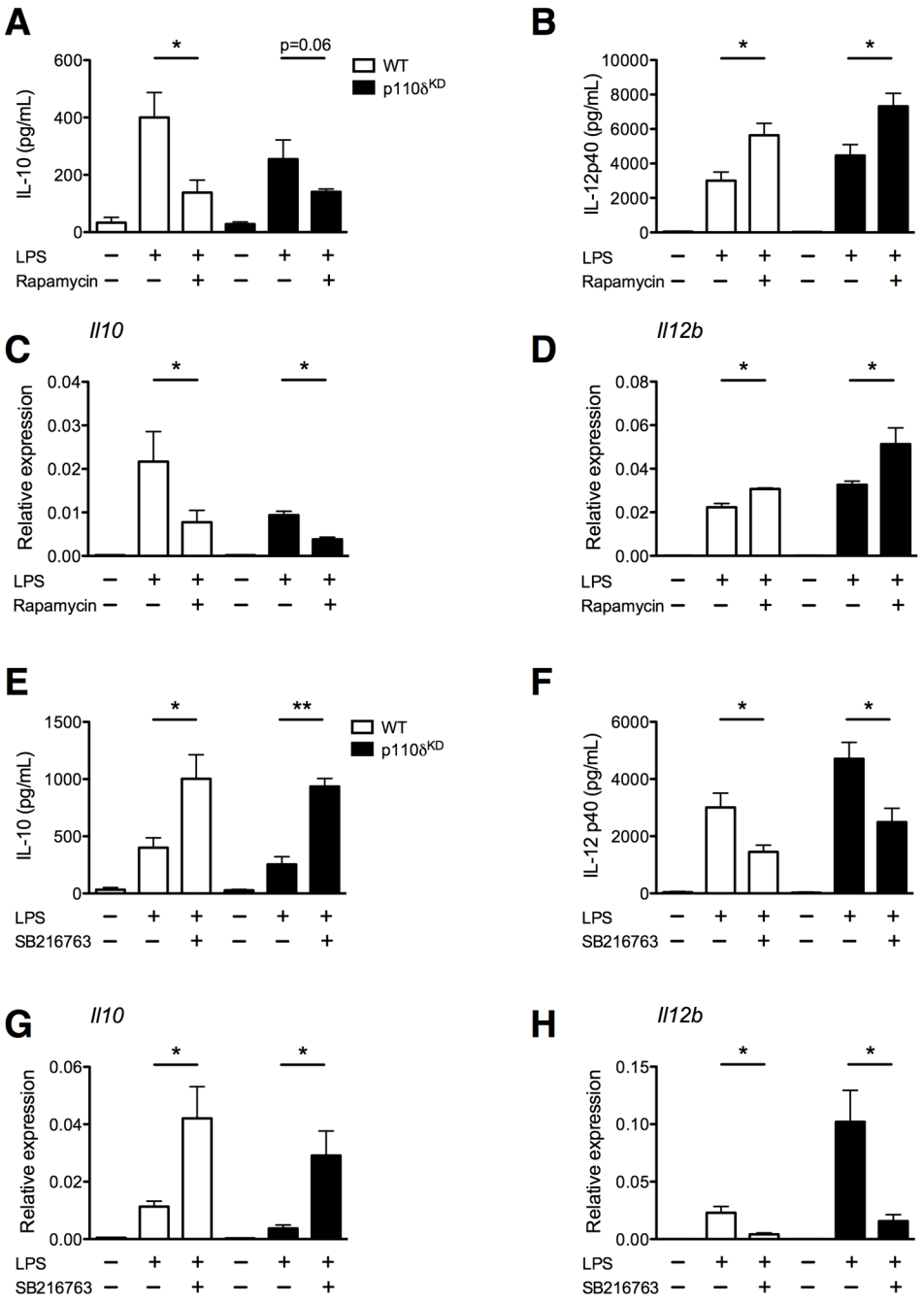

Figure 5. IL-10 and IL-12 p40 production in macrophages is mTOR- and GSK-3β-dependent

WT and p110δ^{KD} BMDMs were cultured with the mTOR inhibitor rapamycin (A-D) or the GSK-3β inhibitor SB-216763 (E-H) for 1 hour prior to stimulation with LPS (1 ng/ml) for 4 (quantitative PCR) or 8 (ELISA) hours. Supernatants were collected and assayed for IL-10 (A, E) and IL-12p40 (B, F) production by ELISA. Error bars represent mean ± SEM from three independent experiments (*, $p<0.05$; **, $p<0.005$). Total RNA was assayed for *Il10* (C, G) and *Il12b* (D, H) expression normalized to *β-actin* expression by quantitative RT-PCR. Error bars represent mean ± SEM from three independent experiments (*, $p<0.05$).

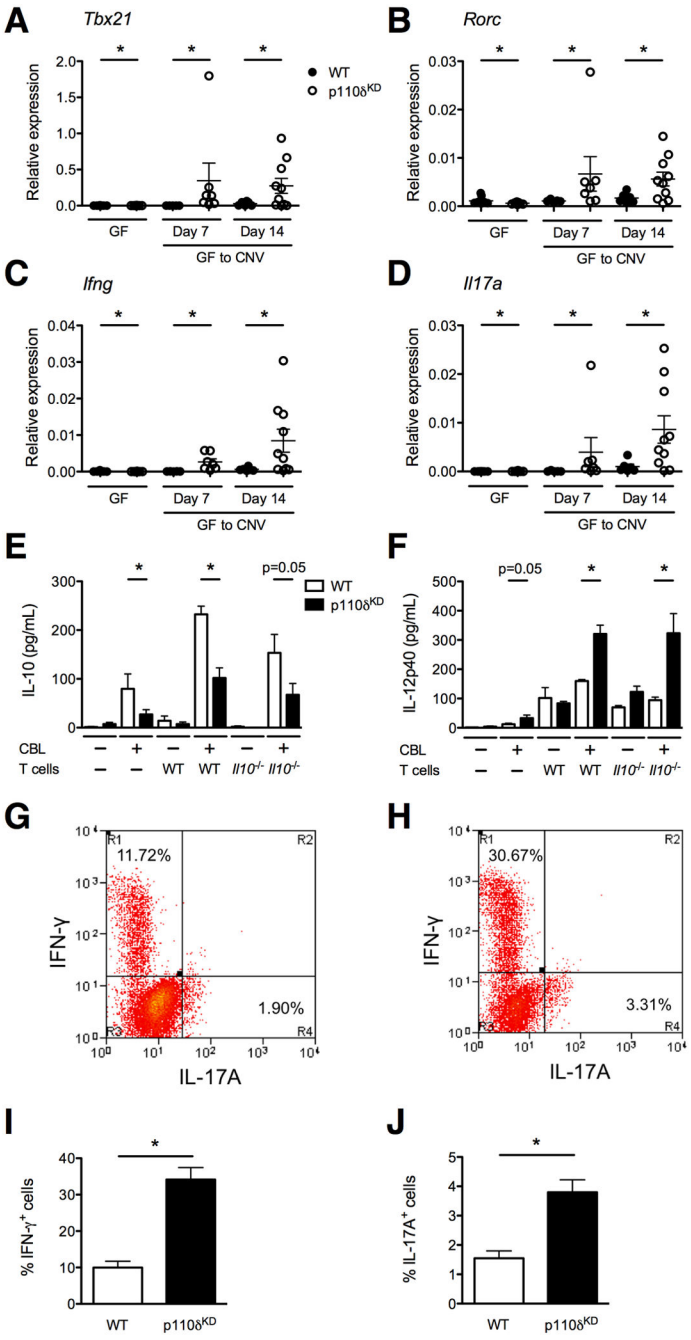

Figure 6. APC p110δ regulates T cell differentiation

(A-D) GF WT and p110δ^{KD} mice were transferred to CNV housing. Colonic tissue was collected from WT and p110δ^{KD} mice sacrificed at days 0 (*n* = 12 and 10, respectively), 7 (*n* = 5 and 7, respectively) and 14 (*n* = 6 and 12, respectively) after transfer. Quantitative RT-PCR was performed in duplicate for *Tbx21* (A), *Rorc* (B), *Ifng* (C), and *Il17a* (D) expression normalized to *β-actin* expression. Error bars represent mean ± SEM (*, p<0.05). (E, F) WT and p110δ^{KD} APCs were cultured overnight with CBL (50 μg/ml) and then co-cultured with WT or *Il10*$^{-/-}$ CD4^{+} T cells at a ratio of 3:2 for 72 hours. Supernatants were

collected and assayed for IL-10 (E) and IL-12p40 (F) production by ELISA. Error bars represent mean ± SEM for three independent experiments (*, $p<0.05$). (G-J) WT and $p110\delta^{KD}$ APCs were stimulated with LPS (10 ng/ml) and OVA peptide (5 μM) overnight and then co-cultured with WT $CD4^+CD62L^+$ OT-II T cells at a ratio of 3:2 for 72 hours. T cells were assayed for IL-17A and IFN-γ production by flow cytometry. $CD4^+$ lymphocytes were gated using forward and side scatter. Representative flow cytometry plots show IFN-γ- and IL-17A-producing WT $CD4^+$ OT-II T cells co-cultured with LPS and OVA stimulated WT (G) and $p110\delta^{KD}$ (H) APCs. Plots are representative of results from three independent experiments with similar results. Quantification of the percentage of total $CD4^+$ T cells producing IFN-γ (I) and IL-17A (J) was determined from the flow cytometry analysis. Error bars represent mean ± SEM from three independent experiments (*, $p<0.05$).

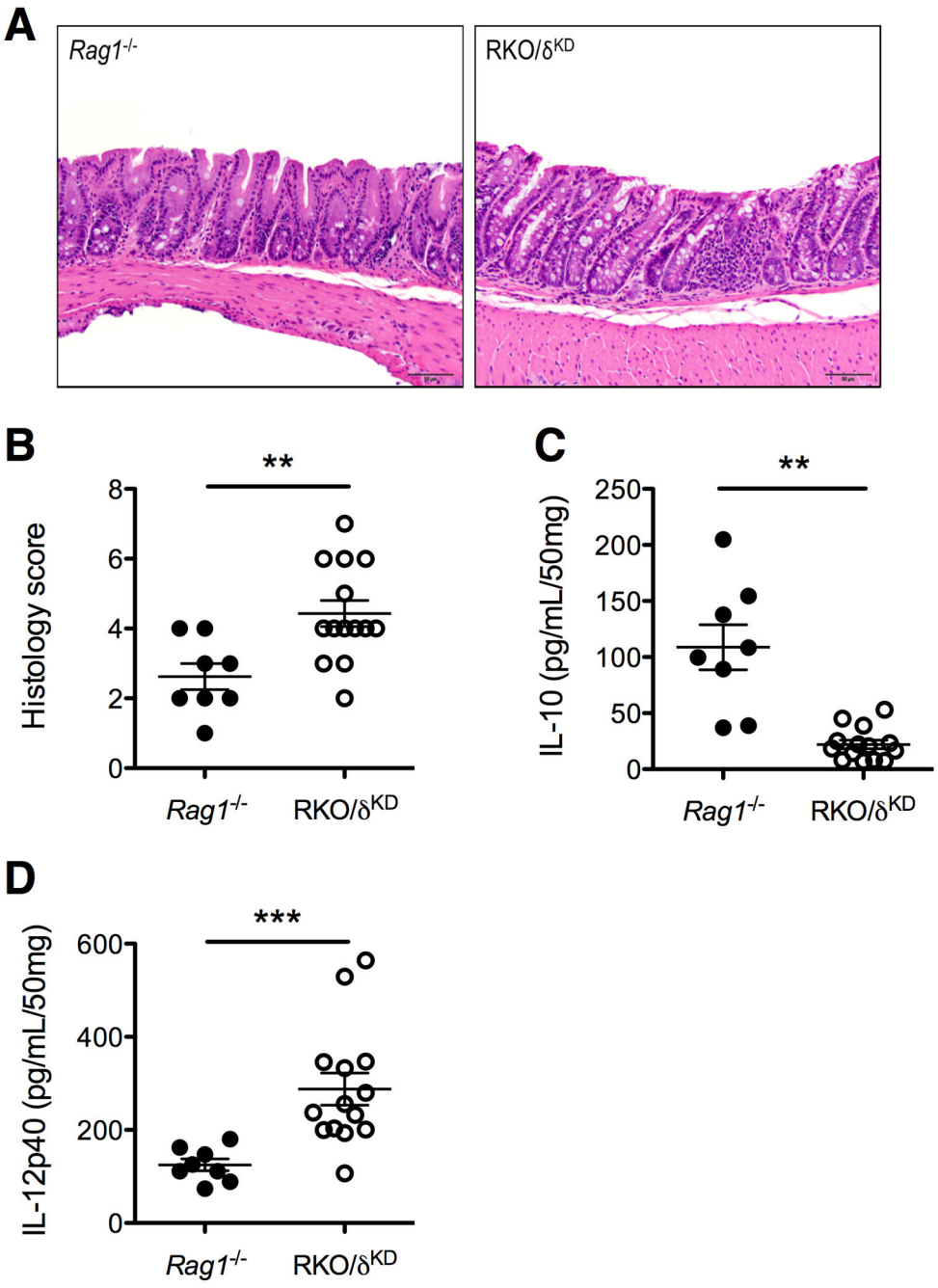

Figure 7. Mild innate mediated colitis develops in *Rag1*$^{-/-}$/p110δ^{KD} (RKO/δ^{KD}) mice

16 week old *Rag1*$^{-/-}$ (*n* = 8) and *Rag1*$^{-/-}$/p110δ^{KD} (RKO/δ^{KD}, *n* = 14) mice were assessed for colitis severity by histopathology and cytokine production in colonic explant cultures. (A) (20X, H&E) Colons from *Rag1*$^{-/-}$ and RKO/δ^{KD} were taken for histological evaluation. Representative sections are shown. (B) H&E slides of colonic tissue were scored for colitis severity using criteria described in the methods by a pathologist (L.B.B.) blinded to the experimental groups. Error bars represent mean ± SEM (**, p<0.005). IL-10 (C) and IL-12p40 (D) production was determined by ELISA and expressed as the amount of

cytokine (pg/ml) per 50 mg colonic tissue weight. Error bars represent mean ± SEM (**, $p<0.005$; ***, $p<0.0005$).

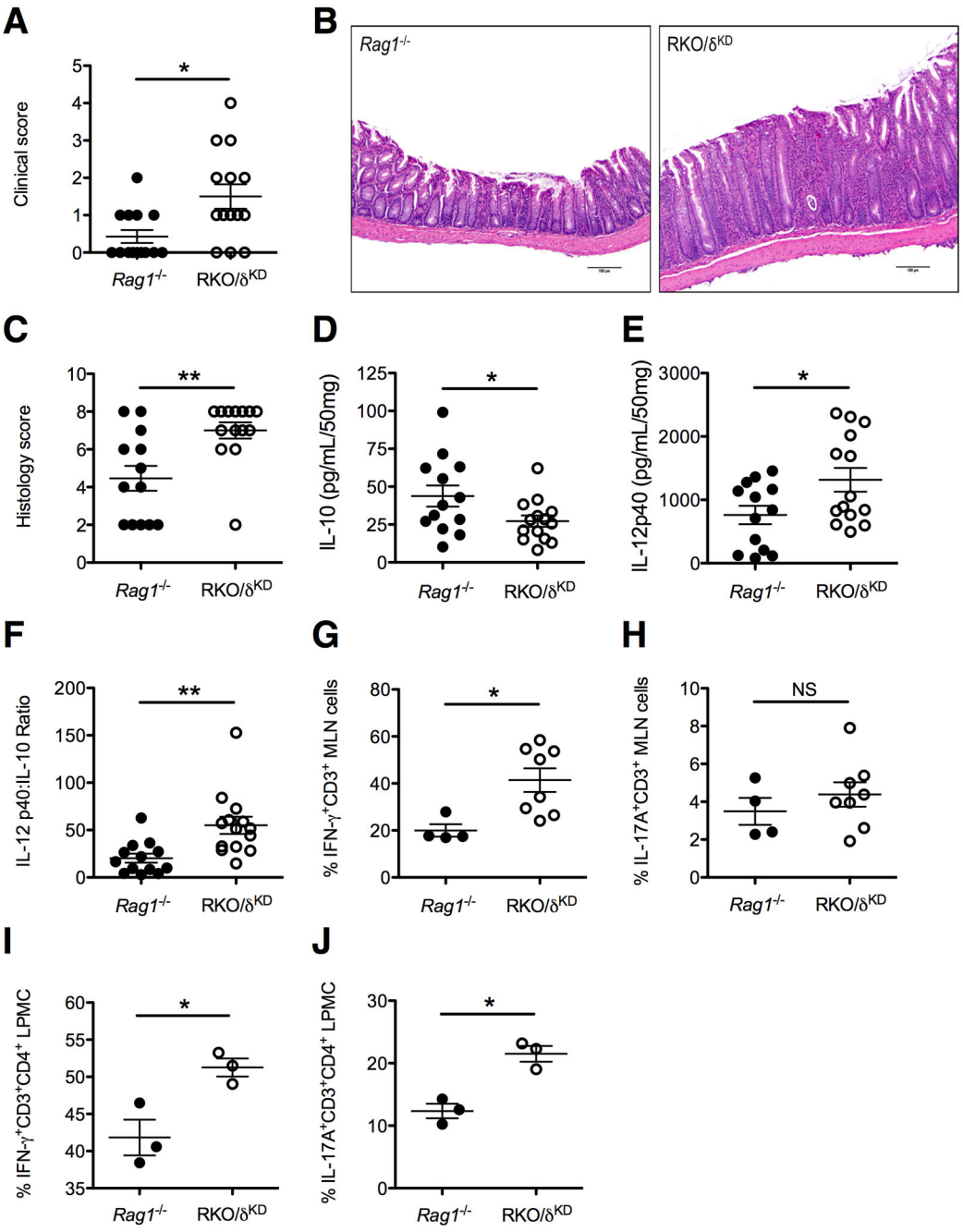

Figure 8. Adoptive transfer of CD4$^+$CD45RB T cells into *Rag1*$^{-/-}$/p110δ^{KD} recipient mice leads to severe colitis

8 week old *Rag1*$^{-/-}$ (n = 13) and RKO/δ^{KD} (n = 14) recipient mice were given 4×10^5 CD4$^+$CD45RB^{high} T cells admixed with 2×10^5 CD4$^+$CD45RB^{low} T cells by i.p. injection to induce colitis as described in the methods. Mice were assessed for colitis severity at 24 days after adoptive transfer. (A) Clinical disease activity scores were determined as described in the methods. Error bars represent mean ± SEM (*, p<0.05). (B) (20X, H&E) Colons from *Rag1*$^{-/-}$ and RKO/δ^{KD} recipient mice were taken for histological evaluation. Representative sections are shown. (C) H&E slides of colonic tissue were scored for colitis severity by a

pathologist (L.B.B.) blinded to the experimental groups as described in the methods. Error bars represent mean ± SEM (**, $p<0.005$). (D-F) Supernatants from 24 hour colonic tissue explants were collected and assayed for IL-10 (D) and IL-12p40 (E) production by ELISA, and are expressed as the amount of cytokine (pg/ml) per 50 mg colonic tissue weight. Error bars represent mean ± SEM (*, $p<0.05$). (F) IL-12p40 and IL-10 protein levels from colonic tissue explant culture in individual mice were used to determine the ratio of IL-12p40 to IL-10. Error bars represent mean ± SEM (**, $p<0.005$). (G, H) Mesenteric lymph nodes (MLNs) from *Rag1*$^{-/-}$ and RKO/δ^{KD} recipient mice were analyzed by flow cytometry for intracellular IFN-γ (G) and IL-17A (H) expression in $CD3^+CD4^+$ T cells. Each point on the graphs represents MLN cells from one mouse. Error bars represent mean ± SEM (NS, not significant; *, $p<0.05$). (I, J) LPMCs were analyzed by flow cytometry for IFN-γ (I) and IL-17A (J) expression in $CD3^+CD4^+$ T cells. Each point on the graphs represents pooled LPMCs from three mice. Error bars represent mean ± SEM (*, $p<0.05$).

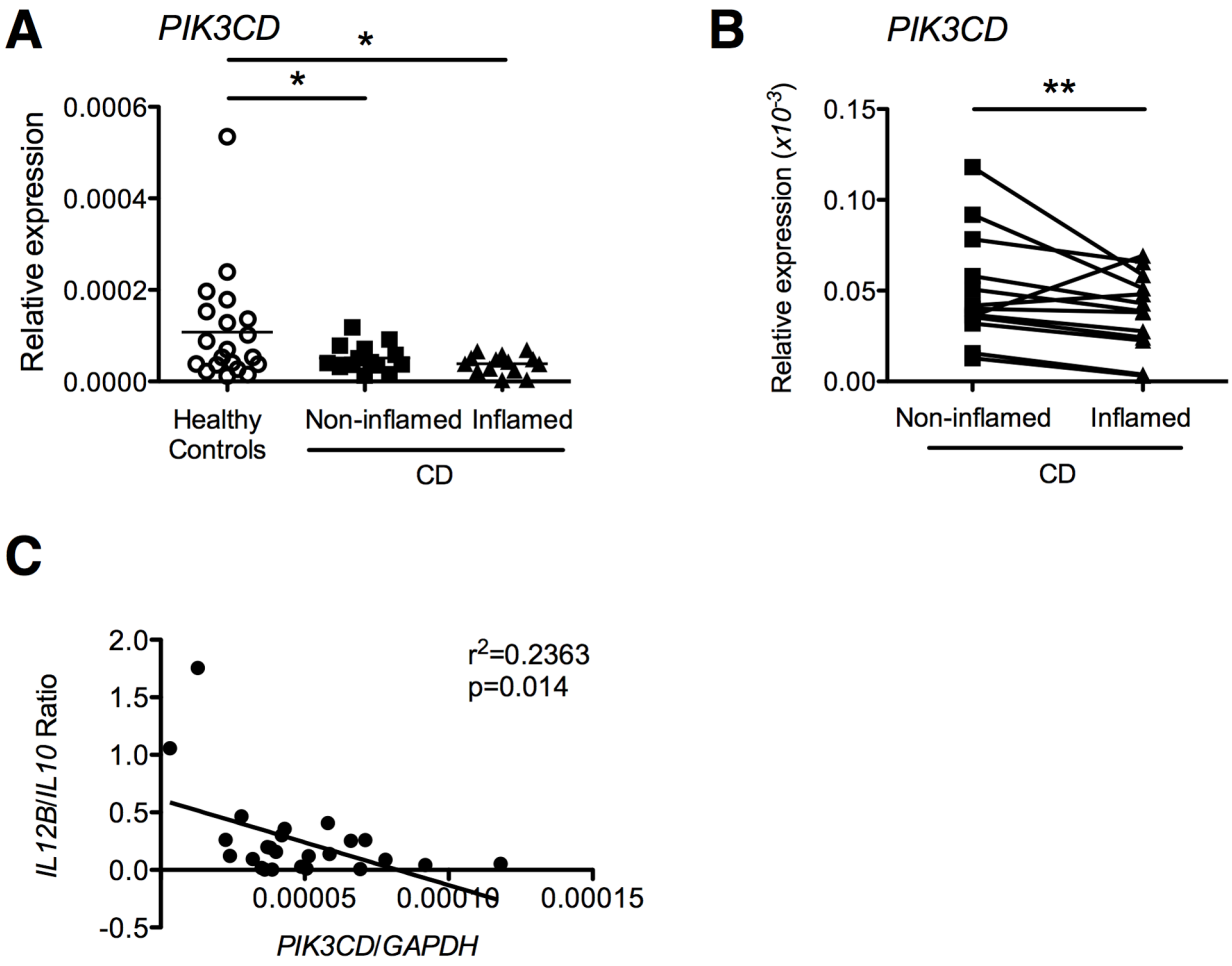

Figure 9. Human intestinal *PIK3CD* expression is decreased in patients with CD and inversely correlates with *IL12B:IL10* ratios

Macroscopically inflamed and non-inflamed colonic or ileal tissue was obtained from patients with CD (*n* = 14) or non-IBD control patients (non-inflamed tissue; *n* = 20) undergoing surgical resection. (A) Total RNA from samples was assessed for *PIK3CD* expression by quantitative RT-PCR in duplicate normalized to *GAPDH* expression. Error bars represent mean ± SEM (*, $p<0.05$). (B) Intestinal *PIK3CD* expression normalized to *GAPDH* expression from patients with CD was assessed at inflamed sites (*n* = 14) and compared to non-inflamed sites (*n* = 14) from the same patient. Lines connect samples from individual patients. Data was analyzed using a paired t test. (**, $p<0.005$). (C) Total RNA from samples was assessed for *IL12B* and *IL10* expression in duplicate normalized to *GAPDH* expression. *IL12B:IL10* ratios in patients were correlated with *PIK3CD* expression ($r^2=0.2363$; $p=0.014$).